Physical Chemistry

Density functional theoretical studies of [2+2] cycloaddition of simple transient silenes and germenes to ethylene, formaldehyde, and thioformaldehyde, and vibrational analysis of spectra of reactants and cyclic products

V. N. Khabashesku, K. N. Kudin, and J. L. Margrave*

Department of Chemistry and Center for Nanoscale Science and Technology, William Marsh Rice University, Houston, TX 77005, USA
Fax: 713 285 5155. E-mail: khval@ruf.rice.edu

The cycloadditions of small unsaturated organic molecules, such as ethylene, formaldehyde, and thioformaldehyde, to simple silenes and their germanium analogues were studied by the density functional theory B3LYP/6-311G(d,p) method. The optimized geometry parameters, vibrational frequencies, and energies of the ground states of the reactants and products and those of reaction transition states found were discussed. A lower reactivity of germenes than silenes in the reactions studied was predicted and a non-concerted two-step mechanism of [2+2] cycloadditions suggested.

Key words: density functional theory method, silenes, germenes, [2+2] cycloaddition, metallacycles, transition states, thioformaldehyde, vibrational analysis, infrared spectra, surface functionalization.

Grafting of organic functional groups to semiconductor surfaces has become an emerging area of research. It is directed to development of new materials with variable opto-electronic properties of covalently attached surface assemblies of organic molecules.[1—4] These materials are used in microscopic electronic devices. Extensive ultrahigh vacuum and wet chemistry studies have been carried out on surface reactivity of group 14 (C, Si, Ge) semiconductors toward small inorganic molecules,[5—9] hydrocarbons,[1] *e.g.*, alkenes[10—17] and aromatics,[18—21] and, most recently, nitrogen-containing polar molecules.[22] The control of chemistry involved in surface functionalization, which produces ultrathin films, is critical for the design of small electronic devices. For this purpose, understanding the way molecules bond to reactive sites on semiconductor surfaces is essential. This knowledge could be especially gained through theoretical modeling of these interactions. In particular, it was succesfully demonstrated by computational studies of [2+2] and [2+4] cycloaddition reactions proceeding on diamond,[23,24] silicon,[10] and germanium[15] surfaces which are reactive due to existing unsaturated C=C, Si=Si, and Ge=Ge dangling bonds. It was found that the reaction patterns of such surface sites closely resemble those known for molecules with π-bonds at carbon, silicon, and germanium atoms

Published in Russian in *Izvestiya Akademii Nauk. Seriya Khimicheskaya,* No. 1, pp. 20—27, January, 2001.

1066-5285/00/5001-0020 $25.00

such as alkenes, disilenes, and digermenes. For example, in the course of chemisorption on silicon, ethylene undergoes [2_s + 2_s] cycloaddition to form surface products with two Si—C σ-bonds in a four-member ring,[16,25] similar to molecular analogues.[26] Relying on these results it is reasonable to imply that the reactions proceeding on surfaces of semiconductors, based on polytypes of silicon carbide SiC and germanium carbide GeC, are likely to parallel the chemistry of molecules containing Si=C and Ge=C double bonds (silenes[26] and germenes,[27] respectively). Thus, theoretical modeling of this chemistry at the molecular level is acquiring practical importance, alongside a principally fundamental interest driving over several decades the research field of multiple bonding to group 14 elements.

Computational methods based on density functional theory (DFT) provide a reliable and economic tool for modeling of reaction dynamics involving silenes and germenes. This was verified, in particular, by our recent theoretical studies of their [2_s+2_s] self-dimerization.[28] The present paper discusses the results of DFT study of cycloaddition of small unsaturated organic molecules, ethylene, formaldehyde, and thioformaldehyde, to simple silenes and their germanium analogues of common formula $R_2M{=}CH_2$ (Scheme 1).

Scheme 1

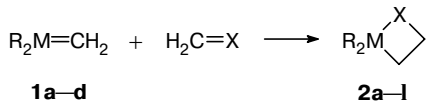

1a—d **2a—l**

1	R	M	**2**	R	M	X	**2**	R	M	X
a	H	Si	**a**	H	Si	CH_2	**g**	H	Ge	O
b	Me	Si	**b**	Me	Si	CH_2	**h**	Me	Ge	O
c	H	Ge	**c**	H	Ge	CH_2	**i**	H	Si	S
d	Me	Ge	**d**	Me	Ge	CH_2	**j**	Me	Si	S
			e	H	Si	O	**k**	H	Ge	S
			f	Me	Si	O	**l**	Me	Ge	S

Theoretical Modeling Procedures

All calculations have been performed with the *Gaussian 94* program[29] running on the NEC SX-3 supercomputer. First, optimized geometries and single-point energies were computed by the RHF method with the the 3-21G basis set. Then the geometries were reoptimized with the 6-311G(d,p) basis set[30] with the density functional theory (DFT)[31] B3LYP[32] method. The harmonic vibrational frequencies were calculated from the analytic second derivatives of the energy at the DFT level. The search for the reaction transition state has been carried out in a way similar to the procedure described in detail previously.[28] The normal mode, corresponding to the imaginary frequency of the molecular structure which represents the transition state, was visualized by the *Xmol* program[33] for SGI computers. The same program was used for performing a full vibrational analysis of the spectra of thioformaldehyde and sila- and germacyclobutanes in the present work.

Results and Discussion

Reactants. The DFT-B3LYP/6-311G(d,p) geometry optimization data and harmonic vibrational frequencies and infrared intensities for the transient silenes **1a,b** and germenes **1c,d** have been documented and discussed in our previous publications.[28,34,35] Both the molecular structures and vibrational frequences for ethylene and formaldehyde are considered firmly established. As for thioformaldehyde, which is a short-lived molecule existing as a monomer in the gas phase under low pressures (with estimated half-life of 6 min at 10^{-2} Torr)[36] or in solid inert matrices at cryogenic temperatures, the full interpretation of its vibrational spectrum is not quite complete.

The IR spectrum of thioformaldehyde generated both by pyrolysis and photolysis of various precursors has been reported in Refs. 37—40 (Table 1). Although a detailed vibrational analysis was done, there still remains an uncertainty about the location of the δ_2 CH_2 scissoring mode.[37—39] The researchers[39] concluded that the δ_2 fundamental is observed in the Ar matrix at 1436 cm^{-1} and it must be overlapped by the strong IR peak of $CH_2{=}CH_2$, present in the matrix as a by-product of $H_2C{=}S$ synthesis. In our recent work[35] we have also detected the spectral bands of matrix-isolated thioformaldehyde in the presence of strong absorptions of $CH_2{=}CH_2$ in the spectra of pyrolysis products of 1,1-dimethyl-1-germa-3-thietane. However, the subtraction of the matrix IR spectrum of authentic ethylene

Table 1. Calculated and observed vibrational frequencies (ν) and calculated intensities (*I*) in the IR spectra of thioformaldehyde and their assignment

ν/cm^{-1} (*I*/km mol^{-1})				Symmetry	Assignment
Experiment			Calculation[d]		
I [a]	II [b]	III [c]			
994	992.8 m	994.4 w	1014 (11)	b_2	$\rho_4(CH_2)$
990	987.4 vs	989.0 vs	1032 (54)	b_1	$\omega_6(CH_2)$
1052	1055.2 m	1064.3 m	1086 (15)	a_1	$\nu_3(C{=}S)$
(1436)	1451.7 w	1449.5 w	1500 (6)	a_1	$\delta_2(CH_2)$
2956	2961.6 s	2963.9 s	3062 (33)	a_1	$\nu_1^s(C{-}H)$
3019	3014.5 m	3017.3 w	3147 (11)	b_2	$\nu_5^{as}(C{-}H)$
2863	2869.0 m	2866.9 w			$2\nu_2$ [e]
	1980.7 w	1985.6 w			$2\nu_6$

Note. Designations: w is weak, m is medium, s is strong band; ρ is rocking, ω is wagging, ν is stretching, δ is scissor vibration; indices "s" and "as" imply symmetrical and asymmetrical vibration.

[a] See Ref. 40.

[b] Ar matrix.[35]

[c] Kr matrix.[35]

[d] B3LYP/6-311G(d,p)

[e] See Refs. 37—40.

from these spectra did not reveal any absorption peaks of the thioformaldehyde that could possibly be obscured by the ethylene band in the 1430-1445 cm^{-1} region. We found instead outside this region a weak band at 1451.7 cm^{-1} in the Ar matrix (1449.5 cm^{-1} in the Kr matrix), which is suggested to be attributed to the δ_2 mode of $H_2C{=}S$. This assignment is in reasonable agreement with the B3LYP/6-311G(d,p) calculated spectrum (see Table 1) and with the interpretation[40] for the observed IR band at 1447 cm^{-1}.

The location of the of the $2\nu_2$ overtone, observed in our recent work[35] as a medium intensity band at 2869.0 cm^{-1} in the Ar matrix (2866.9 cm^{-1} in the Kr matrix), but not as the expected very weak absorption at $1451.7 \cdot 2 = 2903.4$ cm^{-1}, can be explained by the Fermi resonance[41] of this mode with the ν_1 symmetric C—H stretching fundamental of the same (a_1) symmetry. This effect causes the overtone to gain intensity and shifts both vibrational energy levels away from each other by about 40—60 cm^{-1} so that the ν_1 fundamental appears at 2961.6 cm^{-1} in the Ar matrix (2963.9 cm^{-1} in the Kr matrix).

In addition to the previously observed bands,[37—40] a weak absorption band was found at 1980.7 cm^{-1} in the Ar matrix (1985.6 cm^{-1} in the Kr matrix) and assigned to the $2\omega_6$ overtone of the CH_2 wagging mode. Thus, in the present work a full vibrational analysis of the entire set of observed infrared bands for the $H_2C{=}S$ molecule has been completed, as shown in Table 1.

Transition states (TS). The cycloaddition of unsaturated organic molecules $H_2C{=}X$ to metallaalkenes **1a—d** yields four-membered metallacycles **2a—l** according to Scheme 1. Optimized geometries for all transition states found in this study are given on Fig. 1. The structures found have one imaginary vibrational frequency each and thus they represent true transition states. Calculated total energies (E) and ZPE-corrected energies (ZPE is zero-point vibrational energy) for the reactants, transition states, and products are collected in Table 2. A summary of reaction barriers and energies is given in Table 3.

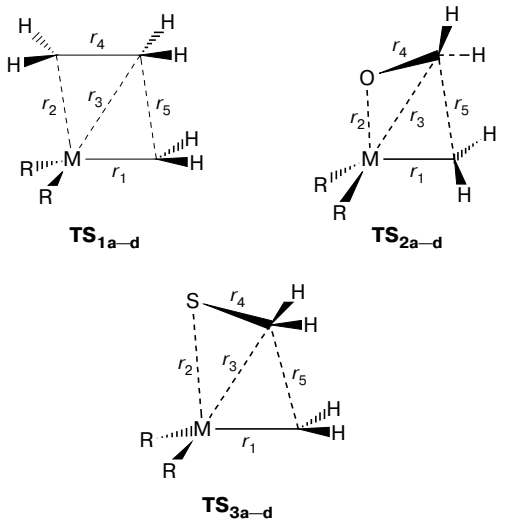

Fig.1 Optimized geometries for cycloaddition transition states found by B3LYP/6-311G(d,p) computation procedure.

Table 2. Calculated B3LYP/6-311G(d,p) total energies (E) and ZPE-corrected energies (E + ZPE) for the reactants, transition states (**TS**), and products of the reactions, and imaginary frequencies (ν) of transition states

Compound, Transition state	E/a.u.	(E + ZPE) /kcal mol^{-1}	ν/cm^{-1}
C_2H_4	−78.61397751	−49299.138	—
$H_2C{=}O$	−114.53633984	−71856.025	—
$H_2C{=}S$	−437.50198377	−274521.153	—
1a	−329.98319644	−207042.483	—
1b	−408.66338797	−256378.496	—
1c	−2117.47161874	−1328709.285	—
1d	−2196.14277982	−1378039.407	—
$\mathbf{TS_{1a}}$	−408.55843689	−256315.740	467
$\mathbf{TS_{1b}}$	−2196.03299538	−1377974.668	584
$\mathbf{TS_{1c}}$	−487.24273083	−305654.825	388
$\mathbf{TS_{1d}}$	−2274.70901198	−1427308.291	492
$\mathbf{TS_{2a}}$	−444.50707165	−278888.727	406
$\mathbf{TS_{2b}}$	−2231.98579305	−1400549.648	431
$\mathbf{TS_{2c}}$	−523.18902856	−328226.768	423
$\mathbf{TS_{2d}}$	−2310.66343235	−1449884.468	460
$\mathbf{TS_{3a}}$	−767.47441466	−481554.405	466
$\mathbf{TS_{3b}}$	−2554.95640591	−1603217.317	235
$\mathbf{TS_{3c}}$	−846.16083113	−530895.117	118
$\mathbf{TS_{3d}}$	−2633.63476199	−1652552.692	208
2a	−408.66544269	−256379.521	—
2b	−487.34551124	−305716.200	—
2c	−2196.14818136	−1378042.836	—
2d	−2274.81886704	−1427373.495	—
2e	−444.61114521	−278949.884	—
2f	−523.29786762	−328290.904	—
2g	−2232.07718893	−1400603.147	—
2h	−2310.75473961	−1449938.099	—
2i	−767.58833163	−481622.760	—
2j	−846.27261131	−530962.094	—
2k	−2555.07329289	−1603287.655	—
2l	−2633.74825049	−1652620.859	—

Table 3. Activation reaction barriers ($\Delta H^{\#}$) and cycloaddition energies (ΔH)

Reactants	Transition state	Reaction product	$\Delta H^{\#}$	ΔH
			kcal mol^{-1}	
$H_2Si{=}CH_2 + C_2H_4$	$\mathbf{TS_{1a}}$	**2a**	25.9	−37.9
$Me_2Si{=}CH_2 + C_2H_4$	$\mathbf{TS_{1c}}$	**2b**	22.8	−38.6
$H_2Ge{=}CH_2 + C_2H_4$	$\mathbf{TS_{1b}}$	**2c**	33.7	−34.4
$Me_2Ge{=}CH_2 + C_2H_4$	$\mathbf{TS_{1c}}$	**2d**	30.2	−35.0
$H_2Si{=}CH_2 + H_2C{=}O$	$\mathbf{TS_{2a}}$	**2e**	9.8	−51.4
$Me_2Si{=}CH_2 + H_2C{=}O$	$\mathbf{TS_{2c}}$	**2f**	7.8	−56.4
$H_2Ge{=}CH_2 + H_2C{=}O$	$\mathbf{TS_{2b}}$	**2g**	15.7	−37.8
$Me_2Ge{=}CH_2 + H_2C{=}O$	$\mathbf{TS_{2d}}$	**2h**	10.9	−42.7
$H_2Si{=}CH_2 + H_2C{=}S$	$\mathbf{TS_{3a}}$	**2i**	9.2	−59.1
$Me_2Si{=}CH_2 + H_2C{=}S$	$\mathbf{TS_{3c}}$	**2j**	4.5	−62.5
$H_2Ge{=}CH_2 + H_2C{=}S$	$\mathbf{TS_{3b}}$	**2k**	13.1	−57.3
$Me_2Ge{=}CH_2 + H_2C{=}S$	$\mathbf{TS_{3d}}$	**2l**	7.9	−60.3

Unlike head-to-tail cyclodimerization of simple silenes and germenes, for which planar symmetric transition states indicating a concerted [2_S + 2_S] reaction path were found by B3LYP/6-311G(d,p) calculations,[28] cycloaddition reactions studied in the present work are likely to follow a non-concerted two-step mechanism. This conclusion came from analysis of the optimized structures of the transition states **TS$_{1a-d}$**—**TS$_{3a-d}$** (see Fig. 1, Table 4) and examination of their calculated imaginary frequencies by computer visualization of corresponding vibrational modes.

According to our calculations, the transition states **TS$_{1a-d}$** for the cycloaddition of ethylene to metallaalkenes **1a**—**d** are all found to have asymmetric planar CMCC ring geometries in which both ethylene carbon atoms are shifted toward the metallaalkene M (Si or Ge) atom. A similar transition state was recently located for the addition of ethylene to silene **1a** by the CASSCF(4,4)/6-31G(d) level of theory, done in an attempt to model the intermediates formed in a reverse reaction — thermal decomposition of silacyclobutane.[42] Unlike these reactions, the transition states **TS$_{1a-d}$**, **TS$_{2a-d}$** for the cycloadditions of formaldehyde and thioformaldehyde are found to be nonplanar with the C—M—O—C and C—M—S—C torsion angles lying within 14.8—32.8°. The ethylene C=C, formaldehyde C=O, thioformaldehyde C=S, silene Si=C, and germene Ge=C bonds are only slightly elongated (as shown by r_1 and r_4 distances in Table 4 and Fig. 1) with respect to those in the parent molecules, indicating that the transition states found nearly repeat the structures of reactants.

Visualization of the vibrational modes corresponding to imaginary frequencies in **TS$_{1a-d}$**—**TS$_{3a-d}$** (see Table 2) has shown them to be primarily associated with ring closing motion along the r_2 stretch. The simultaneous contraction of the r_5 distance takes place at a notably lesser magnitude. This points to the probability of a two-step path from the transition states **TS$_{1a-d}$**—**TS$_{3a-d}$** to four-membered metallacycles **2a**—**l**, proceeding *via* prior formation of M—C, M—O, or M—S bonds in the short-lived C—C broken 1,4-biradical intermediates and their further C—C closing into a ring structure during the second step.

According to the calculated reaction barriers ($\Delta H^{\#}$) and cycloaddition energies (ΔH), the reactions of metallaalkenes **1a**—**d** with ethylene proceed with significantly higher barriers and are less exothermic than the interactions with formaldehyde and thioformaldehyde (see Table 3), in line with the differences in the degree of π-bond polarization in these molecules. For instance, the cycloadditions of germene **1d** to H_2C=S and H_2C=O are calculated to be exothermic by 60.3 and 42.7 kcal mol^{-1}, respectively, and to proceed over barriers of 7.9 and 10.9 kcal mol^{-1}, respectively. In contrast to the cycloaddition to a polar molecule, the barrier for the addition of **1d** to nonpolar ethylene is calculated to be much higher (30.2 kcal mol^{-1}) and this reaction is significantly less exothermic (5.0 kcal mol^{-1}).

Germenes **1c,d** are predicted to be overall less reactive than silenes **1a,b** toward the molecules studied (see Table 3), which correlates with the somewhat weaker Ge=C π-bond *vs.* the Si=C π-bond.[27,35] This is opposite to the established higher reactivity of germenes *vs.* silenes in the reaction of their [2+2] head-to-tail self-dimerization on the basis of experimental[35] and theoretical[28] data. The recent theoretical study[28] has particularly predicted that the dimerization of germene **1d** will proceed with no barrier. In the experimental work[35] the germene **1d** was thermally generated by gas-phase pyrolysis of 1,1-dimethyl-1-germa-3-thietane and trapped along with the by-products, H_2C=S and C_2H_4, in the inert cryogenic matrix. Under conditions facilitating bimolecular reactions, such as an increased pressure (10^{-1} Torr) in the pyrolysis zone or annealing of the matrix to higher diffusion temperatures (35—40 K), only formation of the

Table 4. B3LYP/6-311G(d,p) optimized geometry parameters for transition states **TS$_{1a-d}$**—**TS$_{3a-d}$**

Transition state	M	R	r_1	r_2	r_3	r_4	r_5	Dihedral angle/deg
			Å					
TS$_{1a}$	Si	H	1.766	2.200	2.200	1.406	2.586	0 [a]
TS$_{1b}$	Ge	H	1.848	2.287	2.343	1.411	2.540	0
TS$_{1c}$	Si	Me	1.763	2.257	2.234	1.401	2.561	0
TS$_{1d}$	Ge	Me	1.846	2.346	2.404	1.404	2.502	0
TS$_{2a}$	Si	H	1.771	1.900	2.792	1.258	2.815	32.8 [b]
TS$_{2b}$	Ge	H	1.856	2.122	2.831	1.252	2.628	30.7
TS$_{2c}$	Si	Me	1.769	1.938	2.837	1.258	2.796	24.9
TS$_{2d}$	Ge	Me	1.829	2.409	2.998	1.254	2.402	14.8
TS$_{3a}$	Si	H	1.768	2.720	2.153	1.722	2.648	20.4 [c]
TS$_{3b}$	Ge	H	1.850	2.697	2.264	1.740	2.542	15.3
TS$_{3c}$	Si	Me	1.755	2.884	2.273	1.707	2.667	19.0
TS$_{3d}$	Ge	Me	1.834	2.840	2.394	1.722	2.517	15.6

[a] C—M—C—C.
[b] C—M—O—C.
[c] C—M—S—C.

1,3-cyclodimer of **1d** (and not of cycloadducts **2d** or **2f**) was observed. The present and previous calculation data thus agree well with these experiments, indicating that the dimerization of the germene **1d** is thermodynamically and kinetically more favorable than the cycloaddition of **1d** to $H_2C{=}S$ and to C_2H_4.

Table 5. B3LYP/6-311G(d,p) optimized geometry parameters for metallacycles **2a—l**

Product	Bond length/Å				Bond angle/deg				Dihedral angle/deg
	M—X	X—C	C—C	C—M	C—M—X	M—X—C	X—C—C	C—C—M	
2a	1.901	1.567	1.566	1.902	78.8	87.1	100.8	87.1	29.1
2b	1.905	1.567	1.567	1.907	78.7	87.5	101.1	87.5	28.8
2c	1.997	1.560	1.560	1.997	75.0	88.4	102.5	88.4	27.8
2d	2.002	1.560	1.560	2.002	74.9	88.5	102.7	88.5	28.2
2e	1.687	1.463	1.559	1.888	81.7	93.6	101.6	83.1	0
2f	1.697	1.461	1.555	1.893	81.2	93.6	101.7	83.4	0
2g	1.832	1.451	1.553	1.978	76.1	94.0	103.9	85.4	0
2h	1.845	1.449	1.553	1.984	76.3	94.1	104.1	85.6	0
2i	2.165	1.887	1.555	1.895	83.6	77.8	103.6	95.0	0
2j	2.179	1.885	1.556	1.898	83.1	77.9	103.7	95.4	0
2k	2.266	1.882	1.550	1.984	79.5	78.4	104.8	95.8	25.7
2l	2.280	1.882	1.550	1.990	79.3	78.5	105.2	96.2	26.8

Table 6. Vibrational frequencies (ν) and calculated infrared intensities (I) of vibrations of silacyclobutane and their assignment

ν/cm^{-1} (I/km mol^{-1})				Symmetry	Assignment
Experiment		Calculation			
I [a]	II [b]	(SCF)[46]	(B3LYP)		
{158}[c]	—	163 (0.3)	149 (0.3)	*a′*	Deformation
409 mw	—	455 (9)	416 (7)	*a′*	$\rho(SiH_2)$
514 w	—	557 (0.2)	516 (0.1)	*a″*	$\tau(SiH_2)$; $\tau(CH_2)$ synphase
532 m	532.0 s	589 (27)	541 (21)	*a′*	$\nu^s(SiC)$; (SiH_2)
{653}	651.2 w	702 (4)	642 (2)	*a″*	$\nu^{as}(SiC)$; (SiH_2)
673 m	668.8 m	731 (15)	676 (14)	*a′*	$\rho(CH_2)$
736 m	736.6 m	813 (14)	750 (18)	*a″*	$\rho(CH_2)$ synphase
814 vs	810.0 vs	902 (176)	818 (125)	*a″*	$\omega(SiH_2)$
817 Raman	—	898 (7)	832 (8)	*a′*	$\rho(CH_2)$
877 s	875.0 s	955 (9)	889 (11)	*a′*	Ring puckering
906 s	906.0 m	996 (42)	925 (29)	*a′*	$\rho(CH_2)$
927 s	926.8 m	1026 (35)	946 (19)	*a″*	Asymmetrical ring breathing
962 vvs	963.1 vs	1062 (161)	970 (121)	*a′*	$\delta(SiH_2)$
—	—	1060 (0.1)	989 (0.1)	*a″*	$\tau(CH_2)$ antiphase
—	—	1207 (2)	1096 (1)	*a″*	$\omega(CH_2)$ antiphase
1127 s	1125.0 s	1288 (28)	1162 (22)	*a′*	$\omega(CH_2)$ synphase
1191 mw	1190.0 vw	1323 (2)	1220 (2)	*a′*	$\tau(CH_2)$ synphase
1211 vw	—	1352 (2)	1248 (0.7)	*a″*	$\tau(CH_2)$ antiphase
{1255}[c]	—	1414 (3)	1295 (0.4)	*a″*	$\omega(CH_2)$
1401 m	1398.0 w	1565 (8)	1448 (6)	*a″*	$\delta(CH_2)$ antiphase
1422 m	1417.0 w	1577 (5)	1465 (4)	*a′*	$\delta(CH_2)$ synphase
1458 vvw	1458.0 vw	1622 (0.6)	1499 (1)	*a′*	$\delta(CH_2)$
2145 vvs	2135.0 vs	2314 (172)	2196 (157)	*a′*	$\nu^s(SiH_2)$
2145 vvs	2153.0 vs	2322 (161)	2204 (147)	*a′*	$\nu^{as}(SiH_2)$
2873 m	2865.0 m	3199 (46)	3031 (52)	*a′*	$\nu^s(CH_2)$
—	—	3210 (23)	3049 (3)	*a′*	$\nu^s(CH_2)$ synphase
2888 m	2882.0 m	3205 (40)	3050 (27)	*a″*	$\nu^{as}(CH_2)$
2935 m	2931.0 ms	3248 (26)	3073 (27)	*a′*	$\nu^{as}(CH_2)$
2953 vs	2951.0 m	3271 (22)	3111 (19)	*a″*	$\nu^{as}(CH_2)$
2992 vs	2987.0 ms	3276 (56)	3113 (30)	*a′*	$\nu^{as}(CH_2)$

Note. For designations, see Table 1.
[a] Gas phase.[47]
[b] Ar matrix, 10 K.[48]
[c] Solid phase.[47]

In contrast to these results, the annealing of an Ar matrix containing photochemically generated silene **1b** and formaldehyde resulted in only small amounts of silene dimer and a new reaction product, which was not the expected silaoxetane **2b** but its structural isomer, 2,2-dimethyl-2-silapropanol, with the higher *ab initio* calculated energy.[43] We suggest that such a different course of this reaction could probably be influenced by the higher static pressure built up in the cryogenic matrix cage after photochemical elimination of dinitrogen from the diazocompound[43] used as a silene precursor. Nevertheless, the authors themselves believe that more experiments are necessary to determine whether such a new type of reaction between silenes and formaldehyde is limited only to a solid cryomatrix environment.

Products. According to present calculations, the final products of the cyacloadditions studied, four-membered metallacycles **2a—l**, have either puckered equlibrium structures, as in case of sila- and germacyclobutanes **2a—d** and germathietanes **2k,l** or planar, as sila- and germaoxetanes **2e—h** and silathiethanes **2i,j** (Table 5). Full sets of experimental structural and spectral data are available for comparison with those calculated in the present work only in the case of silacyclobutanes **2a,b**. The computed geometry parameters for **2a** (Table 6) are in close agreement with the gas-phase electron diffraction[44] bond distances (r(Si—C) 1.89 Å, r(C—C) 1.59 Å), valence angles (C—Si—C 80°, C—C—C 100°, Si—C—C 86°, C—C—Si 86°), puckering angle (30±5°), and microwave spectroscopy[45] data (ring puckering angle of ~28°). The B3LYP calculated vibrational frequencies and IR band intensities for **2a** are compared in Table 6 with the previous SCF data[46] and observed spectral bands of **2a** in the vapor phase[47] and in an Ar matrix at 10 K.[48] Although the present B3LYP-DFT calculations agree with the vibrational assignment suggested on the basis of the SCF method,[46] they at the same time provide a closer match between computed and observed vibrational frequencies. The similar accord in computed vibrational frequencies and infrared intensities for 1,1-dimethylsubstituded analogue **2b** and observed IR bands of matrix-isolated **2b** is demonstrated in Table 7. These data thus allow confirmation of the vibrational assignment for **2b** suggested

Table 7. Vibrational frequencies (ν) and calculated infrared intensities (*I*) of vibrations of 1,1-dimethyl-1-silacyclobutane and their assignment

ν/cm^{-1} (*I*/km mol^{-1})		Symmetry	Assignment
Experiment[a]	Calculation[b]		
—	98 (0.3)	*a′*	ρ(SiC_2)
—	141 (0)	*a″*	τ(Me) antiphase
—	159 (0)	*a″*	τ(Me) synphase
—	174 (0)	*a″*	τ(SiC_2)
—	200 (0.9)	*a′*	δ(SiC_2)
—	225 (2)	*a″*	ω(SiC_2)
—	229 (3)	*a′*	Ring puckering
—	447 (7)	*a′*	SiC symmetrical ring puckering
609.0 w	612 (4)	*a′*	ν^s(SiC_2); ρ(CH_2)
—	620 (5)	*a″*	SiC asymmetrical ring puckering; ρ(CH_2) antiphase
648.0 m	652 (11)	*a″*	ρ(CH_2) synphase; ρ(Me) synphase
703.6 m	690 (12)	*a′*	ν^{as}(SiC_2); ρ(Me) synphase
706.1 ms	705 (33)	*a′*	ρ(Me); ρ(CH_2) antiphase
728.0 ms	731 (23)	*a′*	ρ(Me) antiphase; ρ(CH_2) synphase
—	772 (1)	*a″*	ρ(Me) synphase
807.8 m	823 (10)	*a′*	ρ(Me) antiphase; ring puckering
813.2 vs	839 (61)	*a″*	ρ(Me) synphase; ρ(CH_2)
839.7 vs	866 (57)	*a′*	ρ^s(Me)
878.7 vs	901 (65)	*a′*	ν^s(CC); ρ(Me)
905.9 s	920 (53)	*a′*	ρ(CH_2)
921.5 m	945 (14)	*a″*	ν^s(CC)
—	976 (0.1)	*a″*	ρ(CH_2)
—	1093 (0.1)	*a″*	ω(CH_2) synphase
1123.0 s	1160 (35)	*a′*	ω(CH_2) antiphase
1184.0 w	1218 (3)	*a′*	τ(CH_2) antiphase
1214.0 vw	1248 (1)	*a″*	τ(CH_2) synphase
—	1291 (0.6)	*a″*	ω(CH_2)
1248.0 s	1292 (37)	*a′*	δ^{as}(Me)
1254.0 m	1300 (16)	*a′*	ρ^s(Me)
1395.0 w	1448 (10)	*a″*	δ^{as}(CH_2)
—	1457 (0.2)	*a″*	δ(Me)
—	1458 (0.7)	*a′*	δ(Me)
—	1464 (6)	*a′*	δ^s(CH_2)
—	1467 (4)	*a′*	δ^s(Me)
1444.0 w	1472 (6)	*a″*	δ^{as}(Me)
1460.0 w	1497 (2)	*a′*	δ(CH_2)
—	3018 (8)	*a′*	ν^{as}(Me)
—	3020 (11)	*a′*	ν^s(Me)
2852.0 w	3027 (55)	*a′*	ν^s(CH_2)
2871.0 m	3041 (34)	*a″*	ν^{as}(CH_2)
—	3042 (7)	*a′*	ν^s(CH_2)
2933.0 m	3067 (24)	*a′*	ν^{as}(CH_2)
—	3085 (2)	*a″*	ν^{as}(Me)
2965.0 m	3088 (26)	*a″*	ν^{as}(Me)
—	3095 (7)	*a′*	ν(Me)
—	3096 (15)	*a′*	ν(Me)
—	3097 (21)	*a″*	ν^{as}(CH_2)
2982.0 s	3101 (53)	*a′*	ν^s(CH_2)

Note. For designations, see Table 1.
[a] Ar matrix, 10 K.[48]
[b] B3LYP/6-311G(d,p)

earlier without the use of high-level spectra simulations and rely entirely on a comparison with the spectra of related compounds.[48]

The full sets of structural gas-phase electron diffraction (GED), IR spectroscopic and *ab initio* MO calculation data on germacyclobutanes are documented only for the 1,1,3,3-tetramethyl derivative of **2c (3)**.[35,51] However, the endocyclic bond distances Ge—C (1.975 Å) and C—C (1.567 Å), valence angles C—Ge—C (75.3°) and Ge—C—C (89.5°), and ring puckering angle (24°) obtained by GED structure refinement for this compound[51] are comparable with those calculated in the present work for lighter germacyclobutanes **2c,d** (see Table 5). The vibrational assignments of B3LYP calculated spectral features for **2c** and **2d** are given in Tables 8 and 9. The frequencies at 1157 cm^{-1} in **2c** and at 1154 cm^{-1} in **2d**, respectively, calculated to be of me-

Table 8. Vibrational frequencies (ν) and calculated infrared intensities (*I*) of vibrations of germacyclobutane and their assignment

ν/cm^{-1} (*I*/km mol^{-1}) Calculation[a]	Symmetry	Assignment
146 (0.4)	*a′*	Ring puckering
380 (6)	*a′*	ρ(GeH_2)
444 (14)	*a′*	ν^s(GeC); ρ(GeH_2)
485 (0.6)	*a″*	τ(GeH_2); ρ(CH_2) synphase
553 (13)	*a″*	ν^{as}(GeC)
635 (12)	*a′*	ρ(CH_2)
667 (84)	*a″*	ω(GeH_2)
755 (12)	*a″*	ρ(CH_2) synphase; τ(GeH_2)
812 (12)	*a′*	ρ(CH_2) antiphase
877 (88)	*a′*	δ(GeH_2)
879 (17)	*a′*	τ(CH_2) synphase; ν^s(CC)
912 (13)	*a′*	ν^s(CC); ρ(CH) synphase; ρ(CH_2)
961 (5)	*a″*	ν^{as}(CC)
995 (0.02)	*a″*	τ(CH_2) antiphase
1094 (4)	*a″*	ω(CH_2) synphase
1157 (4)	*a′*	ω(CH_2) antiphase
1110—1120 [b]		
1218 (3)	*a′*	ρ(CH_2); τ(CH_2) synphase
1251 (0.7)	*a″*	ρ(CH) synphase
1305 (0.4)	*a″*	ω(CH_2); ρ(CH) antiphase
1454 (4)	*a″*	δ(CH_2) antiphase
1470 (3)	*a′*	δ(CH_2) synphase
1500 (1)	*a′*	δ(CH_2)
2091 (157)	*a′*	ν^s(GeH_2)
2102 (156)	*a′*	ν^{as}(GeH_2)
3024 (56)	*a′*	ν^s(CH_2)
3054 (1)	*a′*	ν^{as}(CH_2)
3059 (38)	*a″*	ν^{as}(CH_2)
3069 (32)	*a′*	ν(CH_2)
3119 (15)	*a″*	ν^{as}(CH_2)
3121 (31)	*a′*	ν^{as}(CH_2)

Note. For designations, see Table 1.
[a] B3LYP/6-311G(d,p).
[b] See Refs. 49 and 50.

Table 9. Vibrational frequencies (ν) and calculated infrared intensities (*I*) of vibrations of 1,1-dimethyl-1-germacyclobutane and their assignment

ν/cm^{-1} (*I*/km mol^{-1}) Calculation[a]	Symmetry	Assignment
96 (0.6)	*a′*	ρ(GeC_2)
117 (0)	*a″*	τ(Me) antiphase
132 (0)	*a″*	τ(Me) synphase
158 (0.2)	*a″*	τ(GeC_2)
169 (2)	*a′*	δ(GeC_2)
170 (2)	*a″*	ω(GeC_2)
198 (3)	*a′*	Ring puckering
400 (7)	*a′*	ν^s(GeC_2)
541 (21)	*a″*	ν^s(GeC_2)
562 (19)	*a′*	ν^{as}(GeC_2)
584 (25)	*a′*	ν^{as}(GeC_2)
628 (21)	*a′*	ρ(CH_2)
649 (2)	*a″*	ρ(CH_2) synphase; ρ(Me) synphase
734 (5)	*a′*	ρ(Me) synphase
785 (3)	*a″*	ρ(Me) synphase
808 (9)	*a′*	ρ(CH_2)
809 (39)	*a″*	ρ(Me) planar
851 (52)	*a′*	ρ(Me) planar
871 (29)	*a′*	τ(CH_2) planar; ρ(CH_2); (CC)
906 (11)	*a′*	ν^s(CC); (CH_2)
960 (5)	*a″*	ν^{as}(CC)
986 (0.3)	*a″*	τ(CH_2) antiphase
1088 (1)	*a″*	ω^{as}(CH_2); (CH_2)
1154 (10)	*a′*	ω^s(CH_2)
1110—1120 [b]		
1132.5 w [c]		
1217 (3)	*a′*	τ(CH_2) synphase; ρ(CH_2)
1250 (0.04)	*a″*	ρ(CH) synphase
1272 (10)	*a′*	ρ(Me) synphase
1280 (3)	*a′*	ρ(Me) antiphase
1302 (0.05)	*a″*	ω(CH_2)
1453 (6)	*a″*	δ^{as}(CH_2)
1462 (0.2)	*a″*	δ^{as}(Me)
1464 (0.5)	*a′*	δ(Me); δ^s(CH_2)
1469 (4)	*a′*	δ^s(CH_2); δ(Me)
1471 (4)	*a′*	δ^s(Me)
1474 (5)	*a″*	δ(Me)
1498 (1)	*a′*	δ(CH_2)
3019 (67)	*a′*	ν^s(CH_2)
3031 (14)	*a′*	ν^{as}(Me)
3032 (11)	*a′*	ν^s(Me)
3046 (2)	*a′*	ν^s(CH_2)
3047 (45)	*a″*	ν^{as}(CH_2)
3060 (34)	*a′*	ν^{as}(CH_2); ν^s(CH_2)
3105 (16)	*a″*	ν^{as}(CH_2)
3106 (1)	*a″*	ν^{as}(Me)
3107 (26)	*a″*	ν^{as}(Me)
3108 (37)	*a′*	ν^{as}(CH_2)
3114 (16)	*a′*	ν^{as}(Me)
3116 (16)	*a′*	ν^{as}(Me)

Note. For designations, see Table 1.
[a] B3LYP/6-311G(d,p).
[b] See Refs. 49 and 50.
[c] Taken from IR spectra of 1,1,3,3-tetramethyl-1-germacyclobutane, Ar matrix, 12 K.[35]

dium oscillator strength in the IR region, are in reasonable agreement with the CH_2 wagging mode, typically observed in the 1110-1120 cm^{-1} region in the IR spectra of ring-unsubstituted germacyclobutanes[49,50] and at 1132.5 cm^{-1} in the ring-substituted derivative **3**.[35] Given the scarcity of literature data on the full spectra of germacyclobutanes and the demonstrated high reliability of the DFT-B3LYP/6-311G(d,p) method in predicting vibrational spectra,[28,35,52] the calculated vibrational frequencies of **2c** and **2d** should provide a valuable source of information for identification of these metallacycles.

Unlike metallacycles **2a—d**, which are stable compounds, the oxa- and thia- metallacyclies **2e—l** exist only as highly reactive intermediates postulated to be formed in pseudo Wittig-type reactions of silenes and germenes with carbonyl and thiocarbonyl compounds.[26,27] Athough the heavier analogues of oxa- and thia- metallacycles have been stabilized due to bulky substituents and studied by X-ray and spectroscopic methods,[26,27] their structural data may not be directly compared with the computed geometry parameters of small cyclic molecules **2e—l** (see Table 4). According to previous theoretical studies,[53] the 1,2-silaoxetane (**2e**), in particular, has not been isolated due to the high exothermicity of the route to ethylene and siloxanes which involves formation of a transient silanone (Scheme 2).

Scheme 2

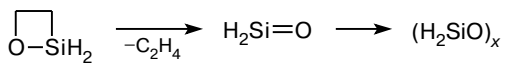

2e

Therefore, one may suggest that the reaction of formalydehyde with the Si=C moiety on the silicon carbide surface could similarly generate surface sites with highly reactive Si=O functions. This example could generally imply the use of the rich chemistry of Ge=O, Ge=S, and Si=S functions in the corresponding metallanones $R_2M{=}X$, arising in the same way as [2+2] cycloreversion of labile metallacycles **2g—l**, for further modification of semiconductor surfaces.

This work has been supported by The Robert A. Welch Foundation of Texas, Mar Chem. Inc., and by the US Army Research Office (Grant No. DAAH04-96-1-0307).

References

1. H. N. Waltenburg and J. T. Yates, *Chem. Rev.*, 1995, **95**, 1589.
2. R. A. Wolkow, *Ann. Rev. Phys. Chem.*, 1999, **50**, 413.
3. *Organics on Semiconductors and Electron Transport. Symp. Proc. 202 ACS Meet.*, *March 2000*, San Francisco, CA, 2000.
4. M. R. Lindford, P. Fenter, P. M. Eisenberger, and C. E. D. Chidsey, *J. Am. Chem. Soc.*, 1995, **117**, 3145.
5. S. M. Cohen, Y. L. Yang, E. Rouchounze, T. Lin, and M. P. D'Evelyn, *J. Vac. Sci. Technol. A*, 1992, **10**, 2166.
6. W. Ranke and J. Wasserfall, *Surf. Sci.,* 1993, **292**, 10.
7. W. Ranke, *Surf. Sci.,* 1995, **342**, 281.
8. T. Lu and J. E. Crowell, *J. Chem. Phys.,* 1993, **98**, 3415.
9. A. Mahajan, B. K. Kellerman, J. M. Heitzinger, S. Banerjee, A. Tasch, J. M. White, and J. G. Ekerdt, *J. Vac. Sci. Technol. A,* 1995, **13**, 1461.
10. R. Konecny and D. J. Doren, *Surf. Sci.,* 1998, **417**, 169.
11. G. T. Wang, C. Mui, C. B. Musgrave, and S. F. Bent, *J. Phys. Chem. B*, 1999, **103**, 6803.
12. A. V. Teplyakov, P. Lal, Y. A. Noah, and S. F. Bent, *J. Am. Chem. Soc.,* 1998, **120**, 7377.
13. S. W. Lee, L. N. Nelen, H. Ihm, T. Scoggins, and C. M. Greenlief, *Surf. Sci.,* 1998, **410**, L773.
14. H. Liu and R. J. Hamers, *J. Am. Chem. Soc.*, 1997, **119,** 7593.
15. P. Lal, A. V. Teplyakov, Y. A. Noah, M. J. Kong, G. T. Wang, and S. F. Bent, *J. Chem. Phys.,* 1999, **110**, 10545.
16. G. P. Lopinsky, D. J. Moffatt, D. D. M. Wayner, M. Z. Zgierski, and R. A. Wolkow, *J. Am. Chem. Soc.,* 1999, **121**, 4532.
17. G. T. Wang, S. F. Bent, J. N. Russell, Jr., J. E. Butler, and M. P. D´Evelyn, *J. Am. Chem. Soc.,* 2000, **122**, 744.
18. R. A. Wolkow, G. P. Lopinsky, D. J. Moffatt, *Surf. Sci.*, 1998, **416**, L1107.
19. G. P. Lopinsky, T. Fortier, D. J. Moffatt, and R. A. Wolkow, *J. Vac. Sci. Technol. A,* 1998, **16**, 1037
20. B. Borovsky, M. Krueger, and E. Ganz, *Phys. Rev. B*, 1998, **57**, R4269.
21. S. Gokhale, P. Trischberger, D. Menzel, W. Widdra, H. Droge, H. P. Steinrück, U. Birkenheuer, U. Gutdeutsch, and N. Rosch, *J. Chem. Phys.,* 1998, **108**, 5554.
22. J. A. Barriocanal and D. J. Doren, *J. Vac. Sci. Technol. A,* 2000, **18**, 1959.
23. M. P. D´Evelyn, In *Handbook of Industrial Diamonds and Diamond Films,* Dekker Publ., New York, 1998.
24. C. Huang, W. Widdra, and W. H. Weinberg, *Surf. Sci.,* 1994, **315**, L953.
25. G. P. Lopinsky, D. J. Moffatt, D. D. M. Wayner, and R. A. Wolkow, *J. Am. Chem. Soc.,* 2000, **122**, 3548.
26. (a) G. Raabe, and J. Michl, *Chem. Rev.,* 1985, **85**, 419; (b) G. Raabe, and J. Michl, in *Chemistry of Organic Silicon Compounds*, Eds. S. Patai and Z. Rappoport, Wiley and Sons, Ltd., 1989, **2**, 1015.
27. (a) J. Barrau, J. Escudie, and J. Satge, *Chem. Rev.,* 1990, **90**, 283; (b) J. Escudie and H.Ranaivonjatovo, *Adv. Organomet. Chem.,* 1999, **44**, 113.
28. (a) K. N. Kudin, J. L. Margrave, and V. N. Khabashesku, *J. Phys. Chem.,* 1998, **102**, 744; (b) V. N. Khabashesku, *Professorial (Dr. Sc. Chem.) Thesis*, N. D. Zelinsky Institute of Organic Chemistry of the Russian Academy of Sciences, Moscow, 1998, 79 pp.
29. M. J. Frisch, G. W. Trucks, H. B. Schlegel, P. M. W. Gill, B. G. Johnson, M. A. Robb, J. R. Cheeseman, T. A. Keith, G. A. Petterson, J. A. Montgomery, K. Raghavachari, M. A. Al-Laham, V. G. Zakrzewski, J. V. Ortiz, J. B. Foresman, J. Cioslowski, B. B. Stefanov, A. Nanayakkara, M. Challacombe, C. Y. Peng, P. Y. Ayala, W. Chen, M. W. Wong, J. L. Andres, E. S. Replogle, R. Gomperts, R. L. Martin, D. J. Fox, J. S. Binkley, D. J. Defrees, J. Baker, J. P. Stewart, M. Head-Gordon, C. Gonzalez, and J. A. Pople, GAUSSIAN 94, Gaussian, Inc., Pittsburg, PA, 1995.
30. (a) R. Krishnan, J. S. Binkley, and J. A. Pople, *J. Chem. Phys.,* 1980, **72**, 650; (b) A. D. McLean, and G. S. Chandler, *J. Chem. Phys.,* 1980, **72**, 5639; (c) M. J. Frisch, J. A. Pople, and J. S. Binkley, *J. Chem. Phys.,* 1984, **80**, 3265.

31. *Modern Density Functional Theory: A Tool for Chemistry*, Eds. J. M. Seminario and P. Politzer, Elsevier, Amsterdam, 1995.
32. (a) A. D. Becke, *J. Chem. Phys.,* 1993, **98**, 5648; (b) C. Lee, W. Yang and R. G. Parr, *Phys. Rev. B,* 1988, **37**, 785.
33. Xmol. Version 1.3.1. Minnesota Supercomputer Center, Inc., Minneapolis, MN, 1993.
34. V. N. Khabashesku, K. N. Kudin and J. L. Margrave, *J. Mol. Struct.,* 1998, **443**, 175.
35. V. N. Khabashesku, K. N. Kudin, J. Tamas, S. E. Boganov, J. L. Margrave, and O. M. Nefedov. *J. Am. Chem. Soc.,* 1998, **120**, 5005.
36. (a) D. R. Johnson and F. X. Powell, *Science*, 1970, **169**, 679; (b) D. R. Johnson and F. X. Powell, and W. H. Kirchhoff, *J. Mol. Spectrosc.*, 1971, **39**, 136; (c) Y. Beers, G. P. Klein, W. H. Kirchhoff, and D. R. Johnson, *J. Mol. Spectrosc.*, 1972, **44**, 553.
37. J. W. C. Johns and W. B. Olson, *J. Mol. Spectrosc.,* 1971, **39**, 479.
38. M. Jacox and D. E. Milligan, *J. Mol. Spectrosc.,* 1975, **58**, 142.
39. O. Watanabe, E. Suzuki, and F. Watari, *Bull. Chem. Soc. Japan*. 1991, **64**, 1389.
40. M. Torres, I. Safarik, A. Clement, and O. P. Strausz, *Can. J. Chem.*, 1982, **60**, 1187.
41. D. C. Harris and M. D. Bertolucci, *Symmetry and Spectroscopy. An Introduction to Vibrational and Electronic Spectroscopy,* Dover Publ. Inc., New York, 1989.
42. L. J. Schaad and P. N. Skancke, *J. Phys. Chem.,* 1997, **101**, 7408.
43. M. Trommer, W. Sander, C.-H. Ottosson, and D. Cremer, *Angew. Chem., Int. Ed. Engl.*, 1995, **34**, 929.
44. L. V. Vilkov, V. S. Mastryukov, V. V. Baurova, V. M. Vdovin, and P. L. Grinberg, *Dokl. Akad. Nauk SSSR,* 1967, **177**, 1084 [*Proc. Acad. Sci., USSR,* 1967, **177**, 1147 (Engl. Transl.)].
45. W. C. Pringle, Jr., *J. Chem. Phys.,* 1971, **54**, 4979.
46. E. T. Seidl, R. S. Grev, and H. F. Schaefer, *J. Am. Chem. Soc.,* 1992, **114**, 3643.
47. J. Laane, *Spectrochim. Acta,* 1970, **26A**, 517.
48. V. N. Khabashesku, A. K. Maltsev, and O. M. Nefedov, *Izv. Akad. Nauk SSSR, Ser. Khim.,* 1980, 837 [*Bull. Acad. Sci. USSR, Div. Chem. Sci.,* 1980, **29**, 591 (Engl. Transl.)].
49. R. Damrauer, *Organomet. Chem Rev.,* 1972, **8A**, 67.
50. P. Mazerolles, M. Lesbre, and J. Dubac, *J. Organomet. Chem.,* 1961, **5**, 35.
51. A. Haaland, S. Samdal, T. G. Strand, M. A. Tafipolsky, H. V. Volden, B. J. J.v.d. Heisteeg, O. S. Akkerman, and F. Bickelhaupt, *J. Organomet. Chem.,* 1997, **536—537**, 217.
52. N. W. Wang, *Chem. Phys. Lett.,* 1996, **256**, 391.
53. S. M. Bachrach and A. Streitwieser, Jr., *J. Am. Chem. Soc.,* 1985, **107**, 1186.

Received July 28, 2000